



Novel assemblies based on oligonucleotides containing intercalating nucleic acid monomers

Asmaa Abdelrahman, Alaa S. Gouda, Per T. Jørgensen & Jesper Wengel

To cite this article: Asmaa Abdelrahman, Alaa S. Gouda, Per T. Jørgensen & Jesper Wengel (2020) Novel assemblies based on oligonucleotides containing intercalating nucleic acid monomers, *Nucleosides, Nucleotides & Nucleic Acids*, 39:1-3, 82-96, DOI: [10.1080/15257770.2019.1683188](https://doi.org/10.1080/15257770.2019.1683188)

To link to this article: <https://doi.org/10.1080/15257770.2019.1683188>



Published online: 01 Nov 2019.



Submit your article to this journal [↗](#)



Article views: 133







View related articles [↗](#)



View Crossmark data [↗](#)



Novel assemblies based on oligonucleotides containing intercalating nucleic acid monomers

Asmaa Abdelrahman^{a,b} , Alaa S. Gouda^{a,c} , Per T. Jørgensen^a , and Jesper Wengel^a 

^aBiomolecular Nanoscale Engineering Center, Department of Physics, Chemistry and Pharmacy, University of Southern Denmark, Odense M, Denmark; ^bDepartment of Photochemistry, National Research Centre, Giza, Egypt; ^cDepartment of Chemistry, Faculty of Science, Benha University, Benha, Egypt

ABSTRACT

This is the first report exploring the capability of twisted intercalating nucleic acid (TINA) and naphthalene-functionalized non-nucleosidic linkers to stabilize and engage in double-helical structures. Four designs were studied with respect to the formation of duplexes and/or other types of self-assemblies. One of the constructs involving TINA provides a thermostable duplex. The biophysical properties of the individual constructs were investigated by UV thermal melting experiments, circular dichroism, and fluorescence emission spectroscopy. Molecular modeling studies were performed in attempts of explaining the biophysical measurements for the duplex based on the TINA-containing oligonucleotide strands.

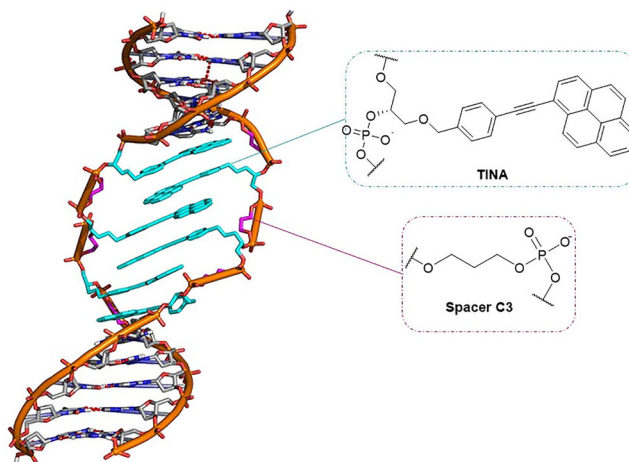
ARTICLE HISTORY



Received 16 September 2019
Accepted 14 October 2019

KEYWORDS

DNA; pyrene; naphthalene;
pi-interactions;
supramolecule

GRAPHICAL ABSTRACT



CONTACT Jesper Wengel  jwe@sdu.dk  Biomolecular Nanoscale Engineering Center, Department of Physics, Chemistry and Pharmacy, University of Southern Denmark, Campusvej 55, 5230 Odense M, Denmark. Color versions of one or more of the figures in the article can be found online at www.tandfonline.com/lncln

In honor and celebration of the 70th birthday of Professor Akira Matsuda

© 2019 Taylor & Francis Group, LLC

Introduction

Modified DNA plays an important role in the biomedical field and has generated significant interest related to possible applications, i.e., relating to drug delivery,^[1] tissue engineering,^[2] nucleic acid-based drugs^[3] and bioimaging.^[4] The modified DNA strands can be designed to engage in different DNA folds or structures, i.e., duplexes, triplexes, quadruplexes and i-motifs.^[5] Besides, DNA has been engineered to form various nano-^[6,7] or micro-sized^[8–10] self-assembled structures. Oligonucleotides (ONs) forming a duplex could be modified with pairs of artificial monomers to provide appealing properties. Thus, such modified ONs not only mimic the supramolecular functions of the natural base pairs but also possess various features that do not reside with the natural nucleic acids. For instance, fluorescence switching ability, the formation of supramolecular aggregates and photo-crosslinking reactions are examples of the reported characteristics of modified duplexes containing pseudo base pairs.^[11]

Similar to the natural nucleic acid duplexes, artificial nucleic acid assemblies can be stabilized via noncovalent forces such as hydrogen bonding, π -stacking, van der Waals and hydrophobic interactions.^[12] The pairs of artificial monomers could stabilize the formed molecular architectures via formation of π -conjugated systems, for example between each other or between the monomer itself and adjacent nucleobases. Several types of aromatic interactions could exist in such contexts, i.e., polar- π stacking, cation- π stacking and π - π stacking.^[13–15] Each kind of aromatic stacking requires certain conditions to be fulfilled, and π - π interaction, for example, occurs only between two aromatic rings when the two planes of the rings stack either face-to-face with an angle between the ring planes less than 30° and the distance between the ring centroids is up to 4.4 \AA , or edge-to-face where the angle between the ring planes is between 60° and 120° and the distance between the rings is at a maximum of 5.5 \AA .^[16,17]

TINA (P) and the so-called M3 naphthalene linker (M3) (Fig. 1) are non-nucleobase monomers that have been reported to partake in many DNA-like

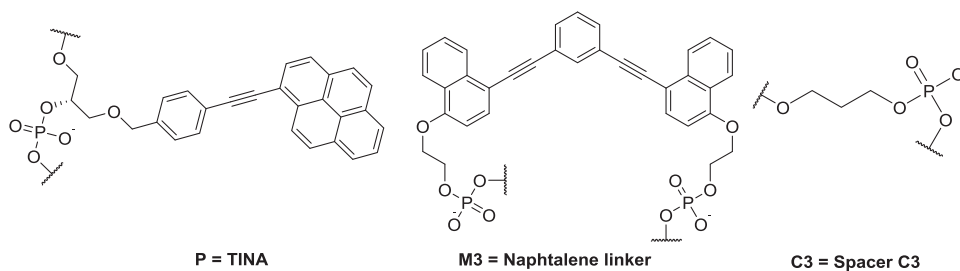


Figure 1. The modifications applied in this study.

Table 1. T_m values of the wild type (wt) and the modified assemblies A1–A4 at 260 nm^a.

ONs	Sequence	Constructs	$T_m \pm 1$ °C
ON01	5'-CTT CCG TGT T-3'	A0 (wt)	43
ON02	5'-AAC ACG GAA G-3'		
ON1	5'-CTT PCP CPG TGT T-3'	A1	N/A ^b
ON2	5'-AAC ACPGPG PAA G-3'		
ON3	5'-CTT M3CM3 CM3G TGT T-3'	A2	N/A ^b
ON4	5'-AAC ACM3 GM3G M3A A G-3'		
ON5	5'-CTP TC3C PCC3 GPT C3GT T-3'	A3	N/A ^b
ON6	5'-AAC PAC3 CPG C3GP AC3A G-3'		
ON7	5'-CTT CCP C3PC3 PC3G TGT T-3'	A4	48 ^c
ON8	5'-AAC ACP C3PC3 PC3G GAA G-3'		

^aConcentration is 2 μ M of each strand in a medium salt buffer (5.8 mM NaH₂PO₄-Na₂HPO₄ buffer, containing 100 mM NaCl and 0.10 mM EDTA).

^bNo transition detected.

^cA second transition recorded three days after mixing of ON7 and ON8.

or DNA-based structures, i.e., triplexes, i-motifs and G-quadruplexes.^[18–21] Also, TINA was incorporated into a DNA scaffold which formed supramolecular assemblies showing photochemical upconversion.^[22,23] In addition, TINA was reported as a promising modified antisense oligonucleotide and was shown to induce exon-skipping in a Duchene muscular dystrophy model.^[24] Additionally, a TINA modification of a G-quadruplex was reported as stabilizing and the resulting structure displayed significant anti-telomerase activity even under molecular crowding conditions.^[25] Also, TINA-modified quadruplexes showed a strong antiproliferative activity in pancreatic cancer cells.^[26]

In addition, the π -conjugating system in TINA and M3 suggests them to be useful as building blocks of supramolecular assemblies via induction of stacking interactions, i.e., π - π stacking, π -polar stacking interactions with water molecules and cation- π stacking interactions with salt ions of the media. Furthermore, the pyrene rings in monomer P or the naphthalene rings in monomer M3 have spectroscopic properties of potential use within biomedical diagnostics.

Herein, eight oligomers (ONs) have been functionalized with unnatural TINA, M3 or C3 spacer monomers in various architectures and designs with the immediate aim of formation of duplex-based structures. Fluorescence spectroscopy, UV thermal denaturation experiments, circular dichroism spectroscopy and gel electrophoresis have been applied to study the formed entities.

Results and discussion

Eight DNA-based oligomers (ON1–8) (Table 1) were synthesized via solid-phase synthesis. The oligomers were designed such that every two strands contain a number of nucleobases which are complementary to each other and thus, in principle, could be hybridized to form modified double-

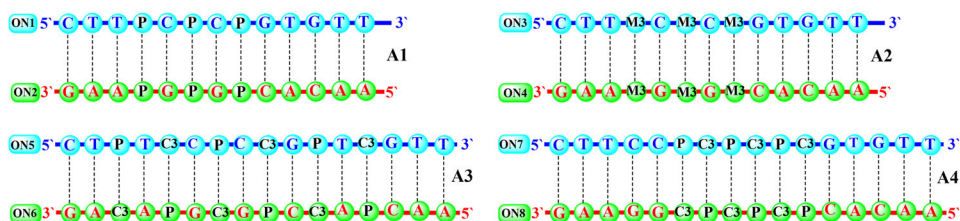


Figure 2. The designs of the modified constructs A1–A4.

stranded helical structures (tentatively assigned as A1–A4, Fig. 2), where A1 possess three P:P pairs, A2 three M3:M3 pairs, A3 six dispersed pairs of P:C3 and A4 six cumulative P:C3 bulged pairs.

Thermal denaturation studies

UV thermal melting experiments were used to indicate duplex formation and to determine the thermal melting temperature (T_m) in the case of formed duplexes. In such an experiment, the prepared sample is heated, while the UV absorbance is continuously recorded.^[27] The assemblies A1–A4 afforded distinct results from thermal denaturation experiments in medium phosphate buffer at pH 7 (Fig. 3A–F). Firstly, the unmodified reference duplex A0 showed a sigmoidal thermal denaturation curve as expected with a T_m value of 43 °C. Mixture A1 showed a hyperchromicity change but no clear sigmoidal thermal denaturation curve. Therefore, it is unlikely that a double-helical structure is formed under these conditions. For A2, a broad sigmoidal thermal denaturation curve was observed though without a significant change in hyperchromicity. Also, in this case, it is most likely that no duplex structure was formed. A similar situation emerged for A3. However, when mixing ON7 and ON8 (mixture A4), a typical sigmoidal thermal denaturation curve with a significant hyperchromicity during heating was observed indicating the formation of a duplex. The thermal denaturation temperature for this complex was increased by 5 °C relative to the reference duplex A0. We envision that the alternating pairs of TINA:C3 and C3:TINA enable interstrand stacking aligned with the stacking and hydrogen bonding involving the nucleobases of the structure. The stability of A4 is intriguing since it has been reported that a TINA monomer destabilizes an anti-parallel duplex due to its extended structure.^[18] Notably, a biphasic curve was recorded for A4 three days mixing of the constituent strands which indicate slow assembly of another structure (Fig. 3F).

Circular dichroism studies

Circular dichroism spectroscopy was used to shed further light on the structures of the complexes A1–A4 (Fig. 4). B-type double-stranded DNA

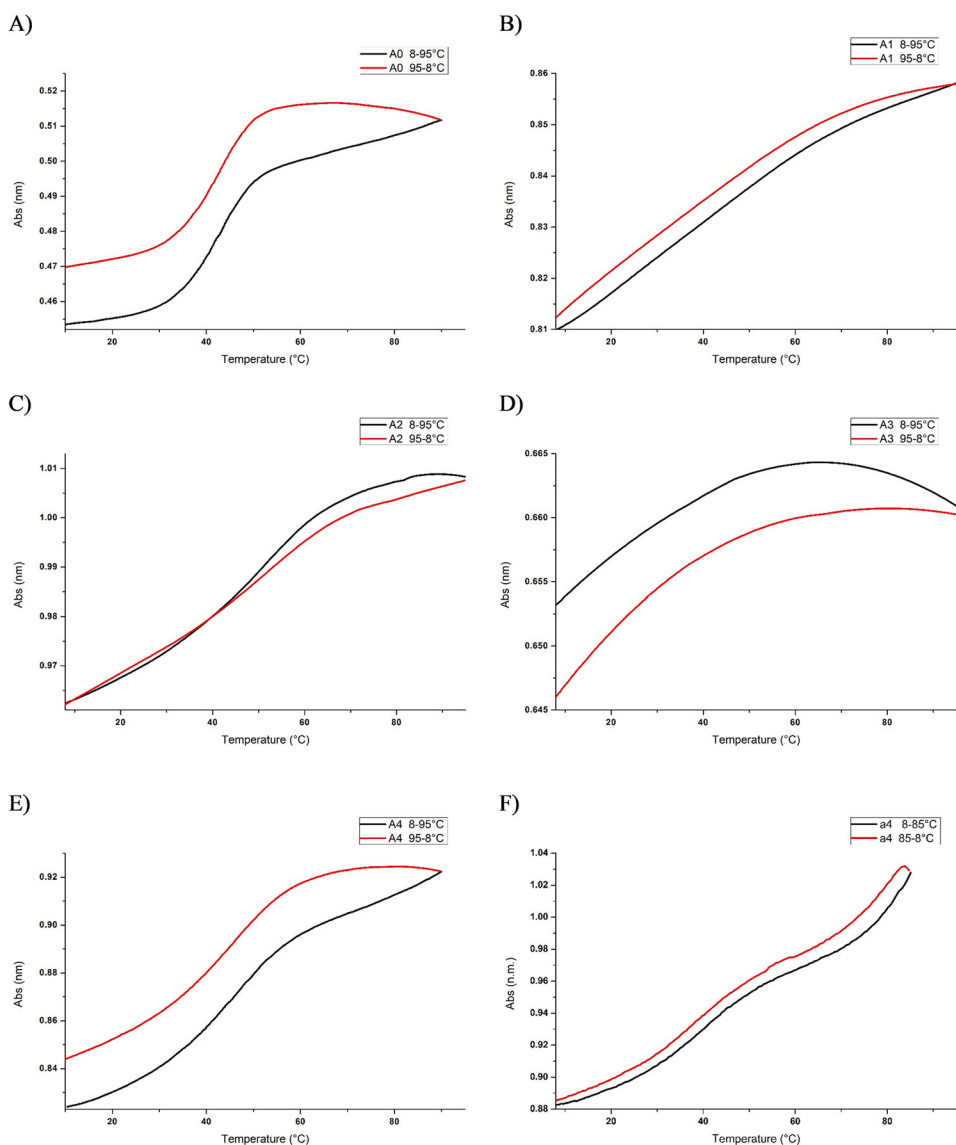


Figure 3. Temperature-dependent UV absorption curves at 260 nm recorded for melting (8–95 °C, black curve) and annealing (95–8 °C, red curve) as follows: A) for the wild type (A0), B–E) T_m curves of freshly prepared modified hybrids A1–A4 subsequently. F) T_m curve recorded three days after mixing ON7 and ON8 (A4).

displays two positive CD bands around 220 and 280 nm in addition to two negative bands around 250 and 205 nm.^[28] Further, stacked chromophores, i.e., pyrene and naphthalene, may display a CD variations, for example via face-to-face stacked pyrenes around 305 nm and face-to-head pyrene interactions around 335 nm.^[29] In addition, cation- π interaction between sodium ions and a π -conjugated system has been reported to induce a signal around 370 nm.^[15,30,31] For A1, the amplitudes of the signals appear

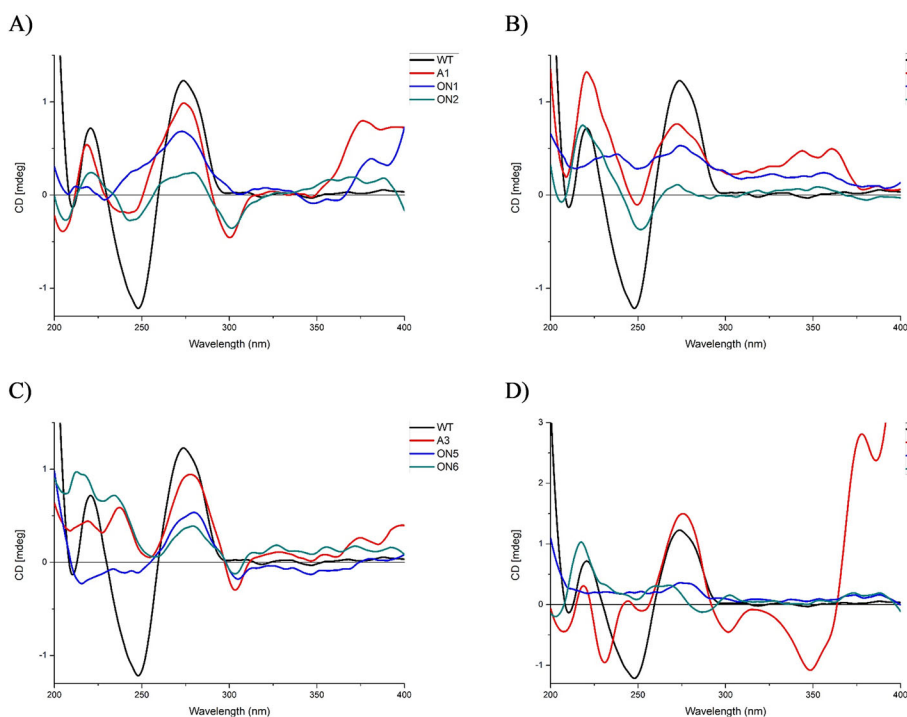


Figure 4. CD spectra of the mixtures A1–A4 (from A to D, respectively) at room temperature; conditions: see Table 1.

simply to be the sum of the individual signals of the two oligomeric constituents, and similar observations were done for A2 and A3. A4, however, displays all the bands characteristic of a B-type duplex structure though with a little blue shifting most likely due to interactions of pyrene units with the adjacent nucleobases (guanine and cytosine) via π -stacking. Furthermore, the interactions of the TINA monomers with the adjacent nucleobases induce positive Cotton effects for the pyrene (observed at 350 nm).^[32] In addition, intensive and distinctive bands originating from interactions between the TINA monomers (at 300 nm) and with ions of the buffer (at 370 nm) are apparent. In summary, the CD experiments strongly support that the mixture A4 is the only one out of the four mixtures that assemble into a duplex structure.

Steady-state fluorescence studies

The four mixtures A1–A4 display luminescence properties due to the TINA and M3 insertions. Since TINA contains pyrene, a fluorescence emission in a free state in the blue light area should be apparent and a green fluorescence signal in a stacked state.^[7,8] Monomer M3 containing naphthalene has been reported to emit fluorescence within the ultraviolet

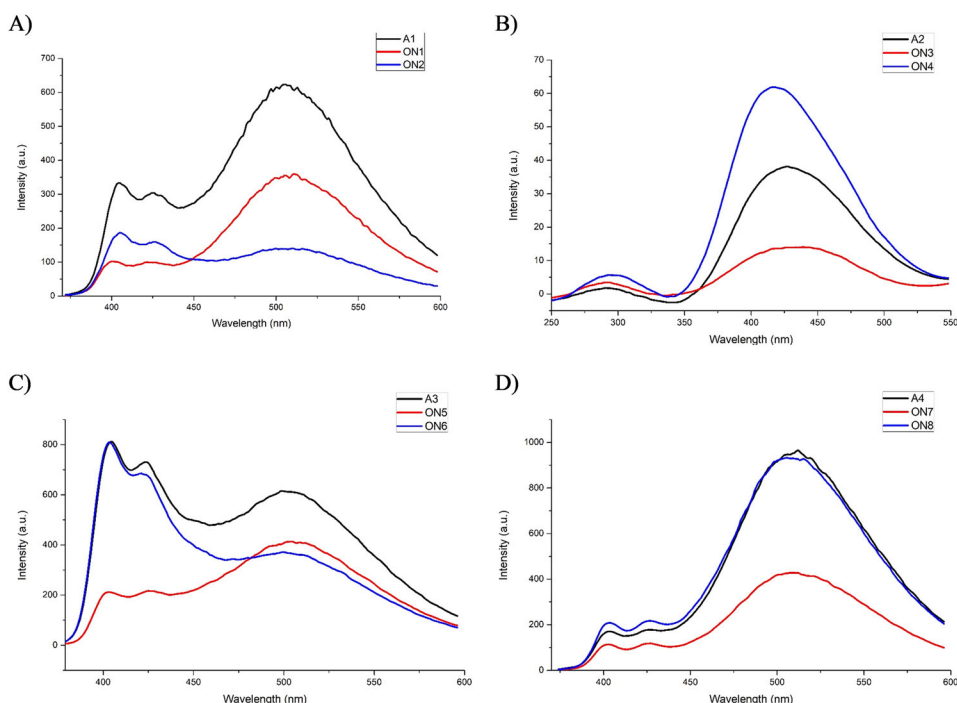


Figure 5. Fluorescence emission spectra of mixtures A1–A4 at room temperature. Excitation: 370 nm, emission range: 380–340 nm; conditions: see Table 1.

light range in a free state, while stacked naphthalenes display a blue emission.^[33,34] Fluorescence emission spectra for A1–A4 and their relevant single strands are displayed in Fig. 5. A1 and A3 and their constituent single-strands display bands typical of pyrene monomer emission (at 405 and 420 nm) and of stacked pyrenes with excimer band at 500 nm. On the other hand, A2 fluorescence emission is quenched which indicates interactions of the naphthalenes of the M3 linker. Mixture A4 shows a degree of quenching, with similar emission intensity as observed for ON8 alone. By comparing the two modified hybrids A3 and A4 (designed to have the same pairs of TINA:C3 and C3:TINA with different insertion positions), we conclude that the insertion positioning affects the ability to form a defined structure.

Polyacrylamide gel electrophoresis

For relatively small nucleic acid strands (<1000 kbp), the electrophoretic mobility is inversely proportional to the molecular weight. Although intercalating monomers such as TINA and M3 could change the mobility of such strands, the fact that negatively charged phosphate linkages are present thorough the constituent strands of A1–A4 make us anticipate that a

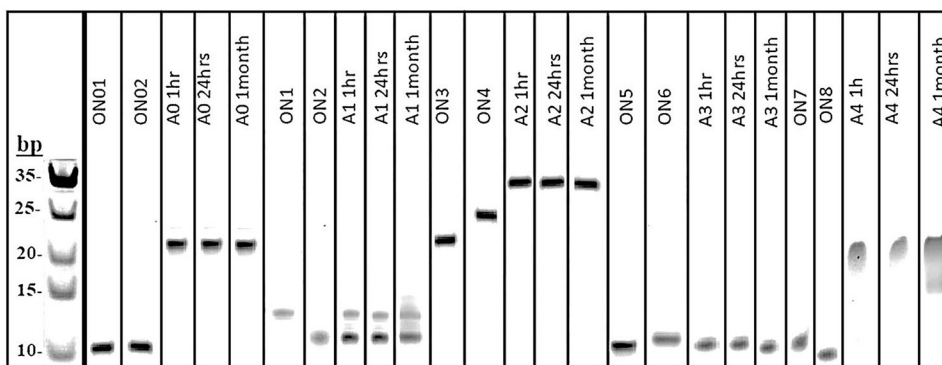


Figure 6. PAGE experiment for 1-hour, 24-hour, and 30-day samples of the four hybrids A1–A4, the wild type A0, and the corresponding single strands. All samples were applied in a total amount of 150 pmol in 10 mM sodium phosphate buffer, 100 mM NaCl and 10% loading buffer, $2 \times$ TBE running buffer, 20% polyacrylamide gel, 2 hour 40 minutes, 20°C , 216 V, 16 mA, 4 W. Left lane: DNA ladder.

similar proportionality exists for these oligomers.^[35] Therefore, PAGE experiments were conducted to examine any aggregation at different time-points after mixing. Fig. 6 provides the PAGE experiment carried out for the four mixtures shortly after mixing of the constituent strands, one day after mixing and 30 days after mixing. As can be seen in Fig. 6, the mobility of the two bands of A1 is a mixture of the single strands ON1 and ON2. The bands for A2 migrate in the region of 35 bp indicating the possible assembly of a polymeric structure, and the single strands ON3 and ON4 show the ability to forming higher-order structures as well. For mixture A3 with six dispersed TINA:C3 bulged pairs, a picture similar to that of the single strands ON5 and ON6 is seen. Mixture A4 with six consecutive pairs of TINA:C3 displays a single band in the same position as the wild-type migrating band which we tentatively assign to the duplex-based structure mentioned above. These gel experiments do not shed light on the explanation of the biphasic T_m curve (Fig. 3F) observed over time.

Molecular modeling

We used molecular modeling in an attempt of rationalizing the assigned duplex-based structure of the A4 construct having six consecutive TINA:C3 pairs positioned into the middle of the duplex. A modified AMBER* force field in Macro Model 9.2 molecular modeling was utilized with the purpose of generating representative low-energy structures. A DNA duplex-based starting structure for A4 was built using standard B-type DNA duplex conformation encompassing the TINA and C3 monomers (see Table 1 for sequences of the involved strands). As can be seen in Fig. 7A,B, the model showed how the TINA moieties may substantially stack on each other.

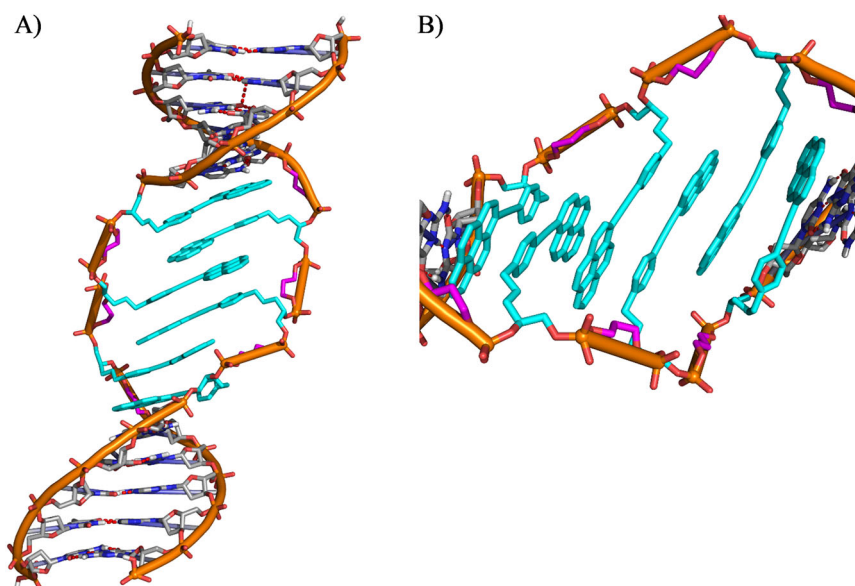


Figure 7. Representative low-energy structure of a 16-mer duplex containing six cumulative TINA:C3 bulged pairs (mixture A4) obtained by an Amber-minimized model. A) Overall view of a possible conformation of A4. The TINA intercalators are marked in cyan, and C3 spacers are marked in magenta. Hydrogen bonds between the canonical nucleobases are depicted in red. B) Side view displaying stacking mode interactions in the central regions of the duplex.

Furthermore, such bulged TINA structures are already stacked with the neighboring nucleobases and thus intercalated between the 10 surrounded base pairs. It seems that the large conjugated TINA moieties enable a rigid fit. A reason for apparent ease of accommodation of the six consecutive TINA:C3 pairs within the duplex structure is the presence of the flexible spacer C3.

Conclusion

Eight oligomers each containing three aromatic modifications plus ten DNA nucleotides have been synthesized. Four of these eight modified oligomers, in addition, contained three spacer C3 monomers. The oligomers have been designed to be complementary in pairs and to allow for interactions between the aromatic monomers.

An unmodified 10-mer all-DNA reference duplex displays a sigmoidal thermal denaturation curve. Three of the four modified complementary oligomer pairs displayed thermal denaturation curves without any clear sigmoidal shape and with only a limited hyperchromic change upon heating. One of the four modified complementary oligomer pair displayed a sigmoidal thermal denaturation curve with thermal denaturation temperature slightly above that of the reference all-DNA duplex. The latter construct

displayed a biphasic thermal denaturation curve after storage at room temperature for three days. The sum of thermal denaturation, CD and fluorescence spectroscopy, gel electrophoresis and molecular modeling experiments supports that exclusively mixture A4 self-assembles into the designed duplex-based structure with a central core of six consecutive TINA:C3 pairs. As a consequence, it is believed that the improved stacking interaction of TINA moieties ascribing to the flexibility of C3 linker intrinsically impacts the duplex biophysical properties. The initial study reported here, investigating the structural effects of various TINA/M3 insertion systems, suggests that the precise placement of nucleobase analog and aromatic linker is critical for duplex formation.

Experimental

Materials and methods

All reagents and solvents have been purchased from commercial suppliers (Sigma-Aldrich, Copenhagen, Denmark). The TINA phosphoramidite (R)-1-O-[4-(1-pyrenylethynyl)benzyl]glycerol was obtained from Innovassynth Technologies (I) Ltd. (Maharashtra, India), the M3 linker from SAPALA Organics Pvt. Ltd. (Telangana, India) and Spacer phosphoramidite C3 from Glen Research (VA, USA). Unmodified DNA sequences ON01 and ON02 were purchased from Sigma-Aldrich (Copenhagen, Denmark).

Synthesis and purification of ON1–ON8

ON1–ON8 were synthesized on an Expedite nucleic acid synthesis system model 8909 from Applied Biosystems (CA, USA) using 4,5-dicyanoimidazole as an activator and an increased deprotection time (98 seconds) and coupling time (9 minutes) for 0.07 M solution of all phosphoramidites in a 1:1 mixture of anhydrous MeCN/CH₂Cl₂. After completion of DNA synthesis, the synthesis columns with CPG supports and DMT-off oligomers were flushed with nitrogen gas. The products were cleaved from the supports by adding 1 mL of a cold and saturated aqueous ammonia solution which was kept at 55 °C for 10 hours. The solution was filtrated and evaporated to dryness under reduced pressure to afford the crude products. Purification of the oligomers was accomplished using reversed phase semi-preparative HPLC (Hitachi 7000; Merck (NJ, USA)) on a LUNA C8 column using a 1:1 mixture of MeCN and Milli-Q water. After collection and evaporation of the pure fraction, the mass of the pure oligomers was confirmed by MALDI-TOF analysis on Bruker's FLEX mass spectrometer and the purity above 90% by analytical HPLC on the machine and using

conditions as described above. Finally, the purified oligomers were quantified by measuring ODs at 260 nm.

Preparation of mixtures A1–A4

The mixtures A1–A4 were obtained by mixing of the two constituent strands in medium phosphate buffer (2 μ M of each oligomer in medium salt of phosphate buffer 100 mM NaCl, 10 mM phosphate buffer system pH = 7) at room temperature; The mixtures were then heated to 90 °C and left to cool at room temperature for 1 hour.

UV spectroscopy

UV spectroscopy was carried out on a Varian Cary 100 or 400 spectrometer (Agilent, CA, USA) using Suprasil[®] quartz cuvette (Hellma, Mülheim, Germany) with pathlength 10 mm at 260-nm wavelength, 1-nm spectral bandwidth and average time of 2 seconds. The thermal denaturation curves for the samples (mixtures A1–A4) were collected, while the temperature was increased with a rate of 0.5 °C/min and data collected at each 0.2 °C temperature step.

Circular dichroism (CD) spectroscopy

The CD spectra of the mixtures A1–A4 were recorded under the same buffer condition as the UV experiments using the CD spectrometer (Jasco J-815, Jasco, MD, USA) using quartz cuvettes with a cell path length of 2 mm at room temperature. The measurements were done in the range from 200 to 400 nm with a continuous scanning mode, a resolution of 0.2 nm and a scanning speed of 50 nm/minute. For each measurement, five spectra were collected and averaged.

Fluorescence spectroscopy

Fluorescence measurements on the mixtures A1–A4 were recorded under the same buffer condition as the UV experiments on a Varian Cary Eclipse spectrometer (Agilent, CA, USA) at an excitation wavelength of 370 nm using quartz Suprasil cuvettes having a 10 \times 4-mm light path with a medium scanning mode using medium voltage. The selection of the emission slit width was 5 nm, and the collected emission spectra were recorded in the range from 380 to 640 nm.

Polyacrylamide gel electrophoresis

Polyacrylamide gel electrophoresis (PAGE) was performed at room temperature using 20% (w/v) polyacrylamide gel containing $2 \times$ TBE buffer and 10% of falcon buffer for loading, 150 pmol of the prepared samples in a 10 mM sodium phosphate buffer and 100 mM NaCl. The gel was pre-run for one hour, and then, the gels were run for 2 hours, 40 minutes at 216 V, 16 mA, 4 W. The polyacrylamide gel was stained for 30 minutes with $1 \times$ SYBRTM Gold from Thermo Fisher (MA, USA) and visualized with a SYNGENE gel imaging box.

Molecular modeling

The initial structure of the assumed TINA-modified DNA/DNA duplex (mixture A4) was generated by building and modifying a standard B-type DNA duplex conformation using MacroModel v9.2, followed by incorporation of six consecutive TINA:C3 pairs into the middle of the duplex. Molecular modeling was carried out with Maestro v9.2 from Schrödinger. All calculations were conducted with AMBER* force field^[36,37] and the GB/SA solvation model^[38] with water parameters as implemented by MacroModel. Non-bonded interactions were treated with extended cutoffs (van der Waals 8 Å and electrostatics 20 Å). The molecular dynamics simulations were performed with stochastic dynamics, a SHAKE algorithm to constrain bonds to H-atoms, time step of 1.5 fs and simulation temperature of 300 K. Simulation for 0.5 ns with an equilibration time of 150 ps generated 250 individual structures, which were minimized using the PRCG method.^[39] During minimization, all atoms were allowed to move freely without freezing with maximum iterations 10000 and convergence threshold of 0.05 kJ/mol in order to attain a relaxed low-energy duplex before applying dynamic simulations described above. The global minimum was used for analysis. A hundred conformations were found for the assumed TINA-modified duplex (mixture A4) within the energy window. Relevant low energy conformers are discussed in the main text of this article. Resulting structures were further processed in PyMOL (v1.7.4.5, 2010. <http://pymol.org>) or in VMD (v1.9.3a6, 2015. <http://www.ks.uiuc.edu>) Molecular Graphics Systems.

Acknowledgments

Joan Hansen and Tina Grubbe Hansen are thanked for technical assistance on oligonucleotide synthesis and purification.

Funding

The VILLUM FONDEN is thanked for funding the Biomolecular Nanoscale Engineering Center (BioNEC), a VILLUM center of excellence, grant number VKR18333. This project has received funding from the European Union's Horizon 2020 research and innovation program under grant agreement No 810685.

ORCID

Asmaa Abdelrahman  <http://orcid.org/0000-0001-5336-3516>

Alaa S. Gouda  <http://orcid.org/0000-0002-8862-4859>

Per T. Jørgensen  <http://orcid.org/0000-0003-3932-5921>

Jesper Wengel  <http://orcid.org/0000-0001-9835-1009>

References

- [1] Ouyang, X.; Li, J.; Liu, H.; Zhao, B.; Yan, J.; He, D.; Fan, C.; Chao, J. Self-Assembly of DNA-Based Drug Delivery Nanocarriers with Rolling Circle Amplification. *Methods* **2014**, *67*, 198–204. DOI: [10.1016/j.ymeth.2013.05.024](https://doi.org/10.1016/j.ymeth.2013.05.024).
- [2] Guven, S.; Chen, P.; Inci, F.; Tasoglu, S.; Erkmén, B.; Demirci, U. Multiscale Assembly for Tissue Engineering and Regenerative Medicine. *Trends Biotechnol.* **2015**, *33*, 269–279. DOI: [10.1016/j.tibtech.2015.02.003](https://doi.org/10.1016/j.tibtech.2015.02.003).
- [3] Udomprasert, A.; Kangsamaksin, T. DNA Origami Applications in Cancer Therapy. *Cancer Sci.* **2017**, *108*, 1535–1543. DOI: [10.1111/cas.13290](https://doi.org/10.1111/cas.13290).
- [4] Zhang, H.; Ma, Y.; Xie, Y.; An, Y.; Huang, Y.; Zhu, Z.; Yang, C. J. A. Controllable Aptamer-Based Self-Assembled DNA Dendrimer for High Affinity Targeting. *Sci. Rep.* **2015**, *5*, 10099. DOI: [10.1038/srep10099](https://doi.org/10.1038/srep10099).
- [5] Yu, Y.; Jin, B.; Li, Y.; Deng, Z. Stimuli-Responsive DNA Self-Assembly: From Principles to Applications. *Chem. Eur. J.* **2019**, *25*, 9785–9798. DOI: [10.1002/chem.201900491](https://doi.org/10.1002/chem.201900491).
- [6] Seeman, N. C.; Gang, O. Three-Dimensional Molecular and Nanoparticle Crystallization by DNA Nanotechnology. *MRS Bull.* **2017**, *42*, 904–912. DOI: [10.1557/mrs.2017.280](https://doi.org/10.1557/mrs.2017.280).
- [7] Laramy, C. R.; Lopez-Rios, H.; O'Brien, M. N.; Girard, M.; Stawicki, R. J.; Lee, B.; de la Cruz, M. O.; Mirkin, C. A. Controlled Symmetry Breaking in Colloidal Crystal Engineering with DNA. *ACS Nano*. **2019**, *13*, 1412–1420. DOI: [10.1021/acsnano.8b07027](https://doi.org/10.1021/acsnano.8b07027).
- [8] Vyborna, Y.; Vybornyi, M.; Häner, R. From Ribbons to Networks: Hierarchical Organization of DNA Grafted Supramolecular Polymers. *J. Am. Chem. Soc.* **2015**, *137*, 14051–14054. DOI: [10.1021/jacs.5b09889](https://doi.org/10.1021/jacs.5b09889).
- [9] Vyborna, Y.; Vybornyi, M.; Rudnev, A. V.; Häner, R. DNA-Grafted Supramolecular Polymers: Helical Ribbon Structures Formed by Self-Assembly of Pyrene-DNA Chimeric Oligomers. *Angew. Chem. Int. Ed.* **2015**, *54*, 7934–7938. DOI: [10.1002/anie.201502066](https://doi.org/10.1002/anie.201502066).
- [10] Vyborna, Y.; Vybornyi, M.; Haner, R. Pathway Diversity in the Self-Assembly of DNA-Derived Bioconjugates. *Bioconjugate Chem.* **2016**, *27*, 2755–2761. DOI: [10.1021/acs.bioconjchem.6b00517](https://doi.org/10.1021/acs.bioconjchem.6b00517).

- [11] Kashida, H.; Asanuma, H. Development of Pseudo Base-Pairs on D-Threoninol Which Exhibit Various Functions. *Bull. Chem. Soc. Jpn.* **2017**, *90*, 475–484. DOI: [10.1246/bcsj.20160371](https://doi.org/10.1246/bcsj.20160371).
- [12] Vengut-Climent, E.; Gómez-Pinto, I.; Lucas, R.; Penalver, P.; Avino, A.; Fonseca Guerra, C.; Bickelhaupt, F. M.; Eritja, R.; González, C.; Morales, J. C. Glucose-Nucleobase Pseudo Base Pairs: Biomolecular Interactions within DNA. *Angew. Chem. Int. Ed.* **2016**, *55*, 8643–8647. DOI: [10.1002/anie.201603510](https://doi.org/10.1002/anie.201603510).
- [13] Li, Q.; Li, Z. The Strong Light-Emission Materials in the Aggregated State: What Happens from a Single Molecule to the Collective Group. *Adv. Sci.* **2017**, *4*, 1600484. DOI: [10.1002/advs.201600484](https://doi.org/10.1002/advs.201600484).
- [14] Li, J.; Du, X.; Hashim, S.; Shy, A.; Xu, B. Aromatic-Aromatic Interactions Enable α -Helix to β -Sheet Transition of Peptides to Form Supramolecular Hydrogels. *J. Am. Chem. Soc.* **2017**, *139*, 71–74. DOI: [10.1021/jacs.6b11512](https://doi.org/10.1021/jacs.6b11512).
- [15] Dougherty, D. A. The Cation- π Interaction. *Acc. Chem. Res.* **2013**, *46*, 885–893. DOI: [10.1021/ar300265y](https://doi.org/10.1021/ar300265y).
- [16] Schrödinger, L. Knowledge Base. New York, NY, 2019, Article ID: 1556- Last Modified: March 30, 2015, accessed May 1 2019. https://www.schrodinger.com/kb/1556?fbclid=IwAR2-R2H0eHc_sLdAXM3tpFznWajzhzrS4o8AKcSvWlWxSdAVmFBsz9oGUAo.
- [17] Hu, Y.; Paterno, G. M.; Wang, X. Y.; Wang, X. C.; Guizzardi, M.; Chen, Q.; Schollmeyer, D.; Cao, X. Y.; Cerullo, G.; Scotognella, F.; et al. π -Extended Pyrene-Fused Double [7]Carbohelicene as a Chiral Polycyclic Aromatic Hydrocarbon. *J. Am. Chem. Soc.* **2019**, *141*, 12797–12803. DOI: [10.1021/jacs.9b05610](https://doi.org/10.1021/jacs.9b05610).
- [18] Bomholt, N.; Osman, A. M.; Pedersen, E. B. High Physiological Thermal Triplex Stability Optimization of Twisted Intercalating Nucleic Acids (TINA). *Org. Biomol. Chem.* **2008**, *6*, 3714–3722. DOI: [10.1039/b808564a](https://doi.org/10.1039/b808564a).
- [19] Geny, S.; Moreno, P. M.; Krzywkowski, T.; Gissberg, O.; Andersen, N. K.; Isse, A. J.; El-Madani, A. M.; Lou, C.; Pabon, Y. V.; Anderson, B. A.; et al. Next-Generation Bis-Locked Nucleic Acids with Stacking Linker and 2'-Glycylamino-LNA Show Enhanced DNA Invasion into Supercoiled Duplexes. *Nucleic Acids Res.* **2016**, *44*, 2007–2019. DOI: [10.1093/nar/gkw021](https://doi.org/10.1093/nar/gkw021).
- [20] Pedersen, E. B.; Nielsen, J. T.; Nielsen, C.; Filichev, V. V. Enhanced anti-HIV-1 Activity of G-Quadruplexes Comprising Locked Nucleic Acids and Intercalating Nucleic Acids. *Nucleic Acids Res.* **2011**, *39*, 2470–2481. DOI: [10.1093/nar/gkq1133](https://doi.org/10.1093/nar/gkq1133).
- [21] El-Sayed, A. A.; Pedersen, E. B.; Khaireldin, N. A. Studying the Influence of the Pyrene Intercalator TINA on the Stability of DNA i-Motifs. *Nucleosides Nucleotides Nucleic Acids* **2012**, *31*, 872–879. DOI: [10.1080/15257770.2012.742199](https://doi.org/10.1080/15257770.2012.742199).
- [22] Mutsamwira, S.; Ainscough, E. W.; Partridge, A. C.; Derrick, P. J.; Filichev, V. V. DNA-Based Assemblies for Photochemical Upconversion. *J. Phys. Chem. B* **2015**, *119*, 14045–14052. DOI: [10.1021/acs.jpcc.5b07489](https://doi.org/10.1021/acs.jpcc.5b07489).
- [23] Mutsamwira, S.; Ainscough, E. W.; Partridge, A. C.; Derrick, P. J.; Filichev, V. V. G-Quadruplex Supramolecular Assemblies in Photochemical Upconversion. *Chem. Eur. J.* **2016**, *22*, 10376–10381. DOI: [10.1002/chem.201601353](https://doi.org/10.1002/chem.201601353).
- [24] Bao, T. L.; Filichev, V. V.; Veedu, R. N. Investigation of Twisted Intercalating Nucleic Acid (TINA)-Modified Antisense Oligonucleotides for Splice Modulation by Induced Exon-Skipping In Vitro. *RSC Adv.* **2016**, *6*, 95169–95172. DOI: [10.1039/C6RA22346J](https://doi.org/10.1039/C6RA22346J).
- [25] Agarwal, T.; Pradhan, D.; Geci, I.; El-Madani, A. M.; Petersen, M.; Pedersen, E. B.; Maiti, S. Improved Inhibition of Telomerase by Short Twisted Intercalating Nucleic

- Acids under Molecular Crowding Conditions. *Nucleic Acid Ther.* **2012**, 22, 399–404. DOI: [10.1089/nat.2012.0372](https://doi.org/10.1089/nat.2012.0372).
- [26] Cogoi, S.; Paramasivam, M.; Filichev, V.; Géci, I.; Pedersen, E. B.; Xodo, L. E. Identification of a New G-Quadruplex Motif in the KRAS Promoter and Design of Pyrene-Modified G4-Decoys with Antiproliferative Activity in Pancreatic Cancer Cells. *J. Med. Chem.* **2009**, 52, 564–568. DOI: [10.1021/jm800874t](https://doi.org/10.1021/jm800874t).
- [27] Wienken, C. J.; Baaske, P.; Duhr, S.; Braun, D. Thermophoretic Melting Curves Quantify the Conformation and Stability of RNA and DNA. *Nucleic Acids Res.* **2011**, 39, e52. DOI: [10.1093/nar/gkr035](https://doi.org/10.1093/nar/gkr035).
- [28] Johnson, W. C. Determination of the Conformation of Nucleic Acids by Electronic CD. In *Circular Dichroism and the Conformational Analysis of Biomolecules*; Fasman, G. D., Ed.; Springer: Boston, MA, **1996**; pp 433–468. DOI: [10.1007/978-1-4757-2508-7_12](https://doi.org/10.1007/978-1-4757-2508-7_12).
- [29] Vyborna, Y.; Altunbas, S.; Vybornyi, M.; Haner, R. Morphological Diversity of Supramolecular Polymers of DNA-Containing Oligopyrenes–Formation of Chiroptically Active Nanosheets. *Chem. Commun.* **2017**, 53, 12128–12131. DOI: [10.1039/C7CC07511A](https://doi.org/10.1039/C7CC07511A).
- [30] Arias, S.; Freire, F.; Quiñoá, E.; Riguera, R. The Leading Role of Cation– π Interactions in Polymer Chemistry: The Control of the Helical Sense in Solution. *Polym. Chem.* **2015**, 6, 4725–4733. DOI: [10.1039/C5PY00587F](https://doi.org/10.1039/C5PY00587F).
- [31] Zhang, H.; Lou, S.; Yu, Z. Polar– π Interactions Promote Self-Assembly of Dipeptides into Laminated Nanofibers. *Langmuir* **2019**, 35, 4710–4717. DOI: [10.1021/acs.langmuir.9b00077](https://doi.org/10.1021/acs.langmuir.9b00077).
- [32] Chen, F. M. Pyrene as a Sensitive Probe for DNA Conformational Changes Due to Protonation. *J. Biomol. Struct. Dyn.* **1983**, 1, 925–937. DOI: [10.1080/07391102.1983.10507494](https://doi.org/10.1080/07391102.1983.10507494).
- [33] Bloyet, C.; Rueff, J.-M.; Cardin, J.; Caignaert, V.; Doualan, J.-L.; Lohier, J.-F.; Jaffrès, P.-A.; Raveau, B. Excimer and Red Luminescence Due to Aggregation-Induced Emission in Naphthalene Based Zinc Phosphonate. *Eur. J. Inorg. Chem.* **2018**, 2018, 3095–3103. DOI: [10.1002/ejic.201800369](https://doi.org/10.1002/ejic.201800369).
- [34] Mendoza, W. G.; Riemer, D. D.; Zika, R. G. Application of Fluorescence and PARAFAC to Assess Vertical Distribution of Subsurface Hydrocarbons and Dispersant during the Deepwater Horizon Oil Spill. *Environ. Sci. Processes Impacts* **2013**, 15, 1017–1030. DOI: [10.1039/c3em30816b](https://doi.org/10.1039/c3em30816b).
- [35] Sigmon, J.; Larcom, L. L. The Effect of Ethidium Bromide on Mobility of DNA Fragments in Agarose Gel Electrophoresis. *Electrophoresis* **1996**, 17, 1524–1527. DOI: [10.1002/elps.1150171003](https://doi.org/10.1002/elps.1150171003).
- [36] Weiner, S. J.; Kollman, P. A.; Case, D. A.; Singh, U. C.; Ghio, C.; Alagona, G.; Profeta, S.; Weiner, P. A. New Force-Field for Molecular Mechanical Simulation of Nucleic-Acids and Proteins. *J. Am. Chem. Soc.* **1984**, 106, 765–784. DOI: [10.1021/ja00315a051](https://doi.org/10.1021/ja00315a051).
- [37] Weiner, S. J.; Kollman, P. A.; Nguyen, D. T.; Case, D. A. An All Atom Force Field for Simulations of Proteins and Nucleic Acids. *J. Comput. Chem.* **1986**, 7, 230–252. DOI: [10.1002/jcc.540070216](https://doi.org/10.1002/jcc.540070216).
- [38] Still, W. C.; Tempczyk, A.; Hawley, R. C.; Hendrickson, T. Semianalytical Treatment of Solvation for Molecular Mechanics and Dynamics. *J. Am. Chem. Soc.* **1990**, 112, 6127–6129. DOI: [10.1021/ja00172a038](https://doi.org/10.1021/ja00172a038).
- [39] Polak, E.; Ribiere, G. Note Sur La Convergence De Méthodes De Directions Conjuguées. *Revue Française D'informatique et de Recherche Opérationnelle. Riro.* **1969**, 3, 35–43. DOI: [10.1051/m2an/196903R100351](https://doi.org/10.1051/m2an/196903R100351).